Response to the reviewer

We thank the reviewer #1 for their useful comments and the time invested in reviewing our manuscript. We have addressed each of the referee comments as detailed point by point below, which we believe has significantly improved the quality of the manuscript.

Reviewer 1

Main Comments

Reviewer Point P 1.1 — P 1.1: There are still undefined parameters in the article: for example what is the value of G?

Reply:

We thank the reviewer for this point. The undefined parameters have been updated in Table 3. The geostropic wind speed (G) is set to around 6.2 m/s, to calibrate the model profile at 573 m, to obtain the required calibration wind speed at a tower height of 100 m.

Reviewer Point P 1.2 — P 1.5: It is great that you have added a grid refinement study. What is the reason that you have not changed the number of cells in the vertical direction? It seems that you have only looked at the influence of the horizontal grid refinement. A proper grid refinement study needs to include all three directions. In addition, the grid refinement study shows some worrying results of the wind speed profiles because the results are not converging with grid refinement (the difference between medium and fine is larger than the difference between coarse and medium. This indicates that you need a finer grid or there is something wrong with the numerical setup. Furthermore, the grid refinement study indicates that your current chosen grid size (the coarsest grid in the grid refinement study) is not sufficient. This is major problem in the article because all the conclusions are based on the results of the coarsest grid.

Reply:

The grid refinement study has been performed, with three different mesh cases and changing the number of cells in all three directions. All the cases that have been run are finer than any case previously used. Previously, due to computational and memory requirements, we had a limit on the number of cells and kept a cap on the number of cells in the vertical direction. The structured grids are generated using the `terrainBlockMesher` tool [2], which interpolates the SRTM terrain data and creates the terrain patch which is blended into a cylindrical domain. The simulation inflow profiles for all the meshes are calibrated to match the field experiment at 100 m of Tower 20 (tse04) on the South-West ridge. A convergence of the wind profiles is seen at towers across the towers on the South-West ridge, inside the valley and on the North East ridge. The simpleFoam (SF1) solver with the $k - \epsilon$ turbulence model setup is utilized for the study. The medium case is chosen for the present mesh study and all the simulations with different models have been re-performed. The mesh resolution cases are well within the recommendations provided by Palma *et al.* [1].

Table 1: Grid refinement study parameters showing the number of cells per main direction.

Case	**Nx**	**Ny**	**Nz**	**NCells (million)**
Coarse	550	550	150	62
Medium	600	600	170	88
Fine	650	650	190	115

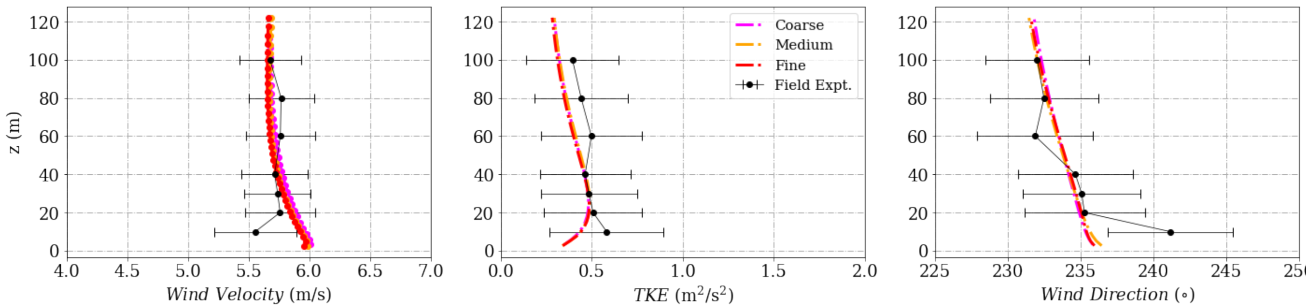

Figure 1: a) Wind velocity magnitude b) Wind direction c) Turbulent kinetic energy tuned to reach calibration at height 573 m corresponding to 100 m at Tower 20 (tse04)

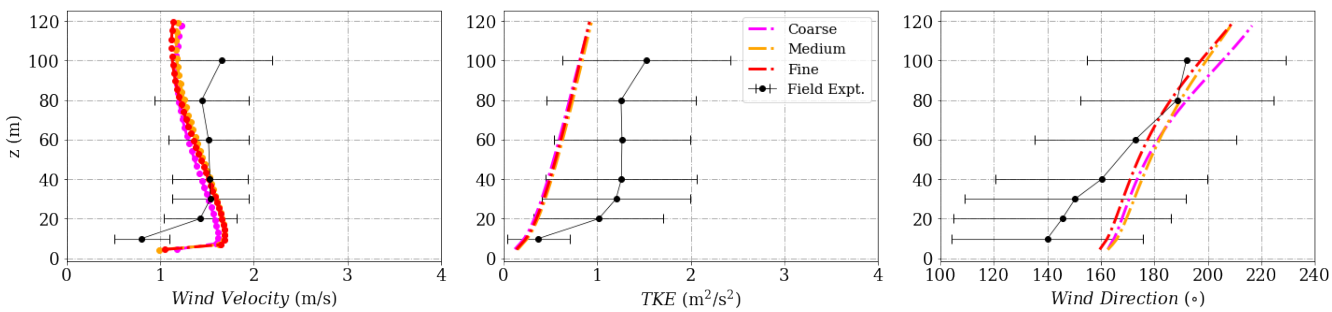

Figure 2: a) Wind velocity magnitude b) Wind direction c) Turbulent kinetic energy at Tower 25 (tse09)

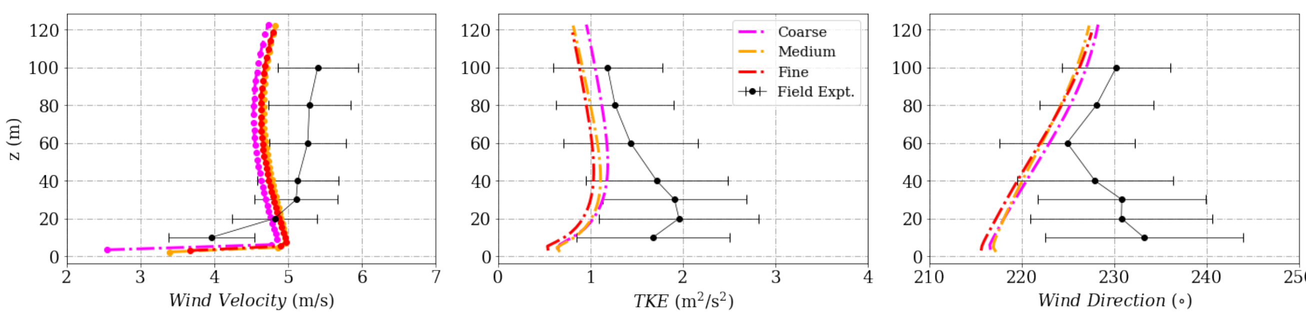

Figure 3: a) Wind velocity magnitude b) Wind direction c) Turbulent kinetic energy at Tower 29 (tse13)

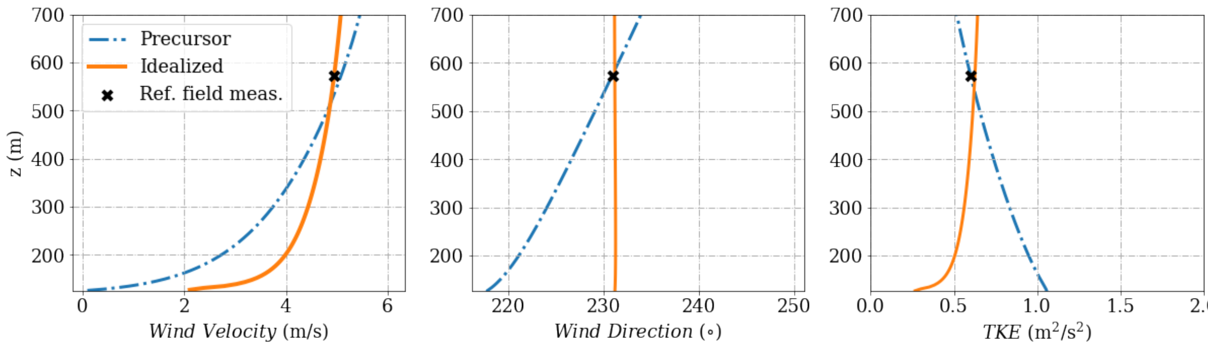

Figure 4: Idealized and Precursor (developed) input profiles for a) Wind velocity magnitude b) Wind direction c) Turbulent kinetic energy tuned to reach calibration at height 573 m corresponding to 100 m at Tower 20 (tse04)

Reviewer Point P 1.3 — P1.6: Great that you have added results for the inflow profiles. It seems that the ABL setup (with Coriolis and ABL height) under predicts the TKE (or TI) by quite a margin, which makes a comparison/validation with measurements challenging. You could actually find a set of G and ℓ_{max} that gives you a matching TI at a reference height (as long as the TI value exist for a given z_0 and G). See for example the Appendix of a recent work of my own [1]. If you cannot get a matching TI, then you could choose to change the roughness height for the ABL inflow.

Reply:

Yes, the ABL setup (with Coriolis and ABL height) indeed underpredicted the TKE. We have addressed this issue by increasing the roughness length z0 of the precursor, while also tuning pressure gradient magnitude and direction to get the right wind speed, wind direction, and now TKE at the reference height to match the met mast average values. The z0 was only increased in the precursor setup to 6 (m), such that the successor setup still uses a z0 matching the average value in the complex terrain patch. The new tuned values for pressure gradient magnitude and direction used in the precursor was also used for the successor simulations. Increasing the TKE at the inlet notably altered the flow structure inside the valley, which is evident when comparing the new updated LIC figures, Figure 15 (b), to the one submitted in the previous version.

Reviewer Point P 1.4 — P1.7: You mention that you focus on the influence of the source terms; however, you do validate and evaluate the performance of each the model with the measurements throughout the article and in the conclusion. Hence, I think it makes sense to perform a range of wind wind directions and apply a Gaussian filter as post processing step, especially if the wind direction standard deviation is as large as $7°$. You could at least perform two additional wind directions representing the standard deviation $(231 \pm 7°)$ and look at the difference between the three wind directions.

Reply:

We agree with the reviewer on this point. The inflow direction plays an essential role in the wind predictions for complex terrains. A wind direction standard deviation of around $7°$ is seen in the field measurements at Tower 20 (tse04). Simulations have been performed for two additional wind directions $(231 \pm 3.5°)$ for each model to look at the differences observed between the three incoming wind directions. The results have been discussed in the Results in Section 4.4 and in Appendix for the wind profiles at three different met-masts, corresponding to Tower 20 (tse04) on the South-West ridge, Tower 25 (tse09) inside the valley and Tower 29 (tse13) on the North-East ridge in Sections 1.

1 SF1 $k - \epsilon$

All simulations are calibrated for Tower 20 as seen in Fig 6 with the same inflow velocity at the reference height of 100 m on the tower and only changing the wind direction. The predicted profiles inside the valley and on the North-East ridge appear to vary quite significantly with the inflow wind direction as seen in Figs 7 and 8. Streamline trajectories for the inflow with three different wind directions at the Towers are shown in Fig 5. Wind passing through Tower 29 with inlet wind from 234.5° exhibits a very different trajectory compared to the other inlet wind directions and the set of trajectories passing through the mast upstream, Tower 20. The wind here was initially deflected off from the NE ridge and led into the valley by a channelling effect. As a result, the wind speed decreases significantly before passing Tower 29, before re-gaining in intensity downstream of the ridge as the wind accelerates downhill.

2 SF2 $k - \omega$

The influence of wind direction change using the SF2 $(k - \omega)$ model at different towers is shown in Figs 9, 10 and 11 respectively. The results appear to be similar to the SF1 $(k - \epsilon)$ model. However in comparison a lesser difference is seen in the profiles between the $231°$ and the $234.5°$ degree cases at Towers 25 and 29.

3 SF3 Canopy

The influence of wind direction change using the SF3 (Canopy) model at different towers is shown in Figs 12, 13 and 14 respectively. A much larger difference in wind profiles is seen at Tower 29 on the North-East ridge compared to the SF1 $(k - \epsilon)$ model indicating larger uncertainties with wind direction. Presently, the canopy is modeled using a uniform tree height, and perhaps there would be higher uncertainties with a non-uniform canopy across the domain, the path taken by the wind for different inflows would vary significantly. A much different re-circulation zone is developed, as seen in the wind direction profiles.

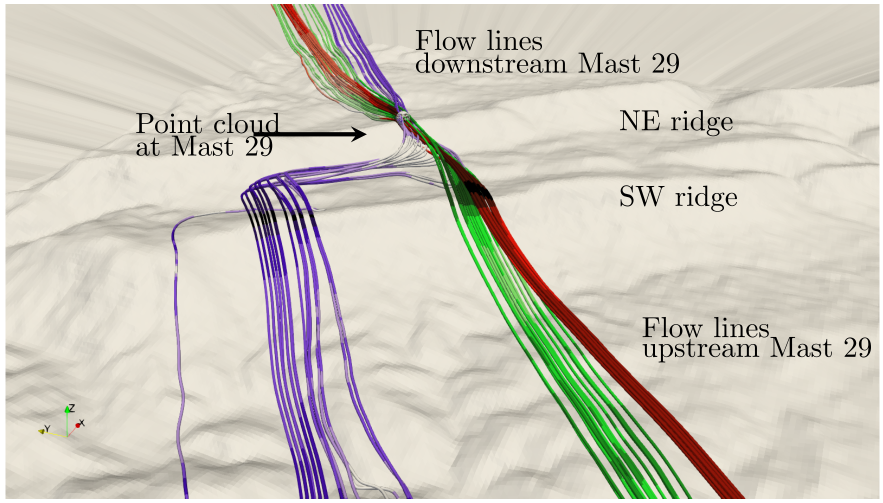

(a) Mast 29.

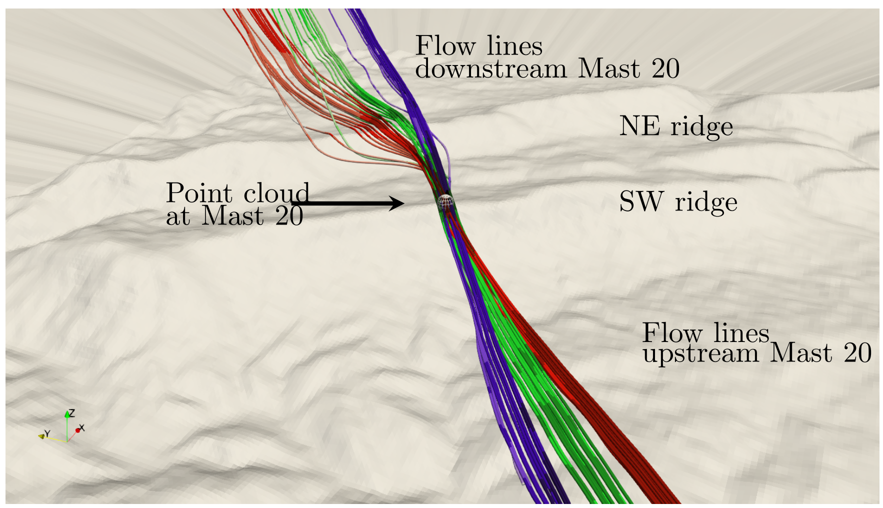

(b) Mast 20.

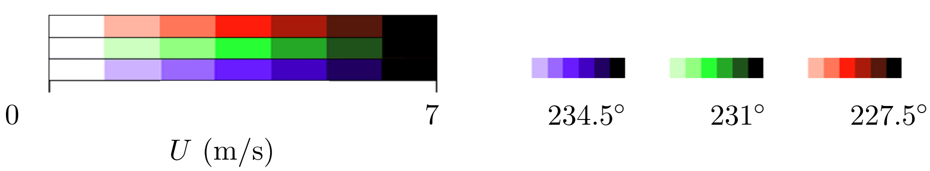

Figure 5: Wind paths of air parcels passing through a sphere of 55 m radius placed on top of the ground at given met mast locations. Flow lines colored in green represent trajectories for wind coming from 231° at the inlet, while red and blue lines illustrate wind at the inlet from 227.5° and 234.5° correspondingly.

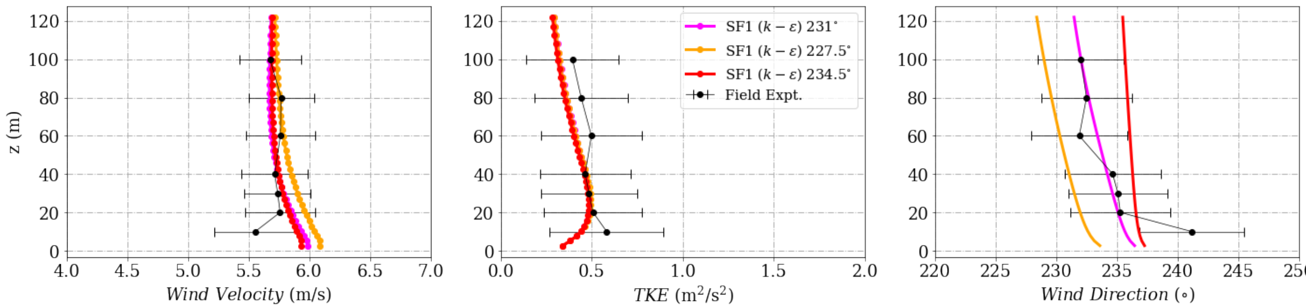

Figure 6: Simulation results and experimental data for wind velocity on the Southwest ridge at Tower 20 (tse04) for for the SF1 ($k-\epsilon$) model. The locations of the masts are given in Fig **??**.

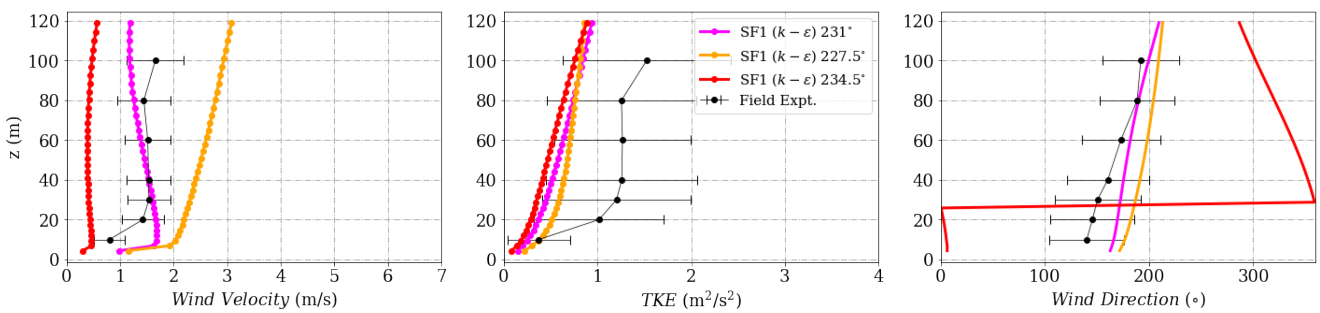

Figure 7: Simulation results and experimental data wind velocity inside the valley at Tower 25 (tse09) for the SF1 ($k-\epsilon$) model.

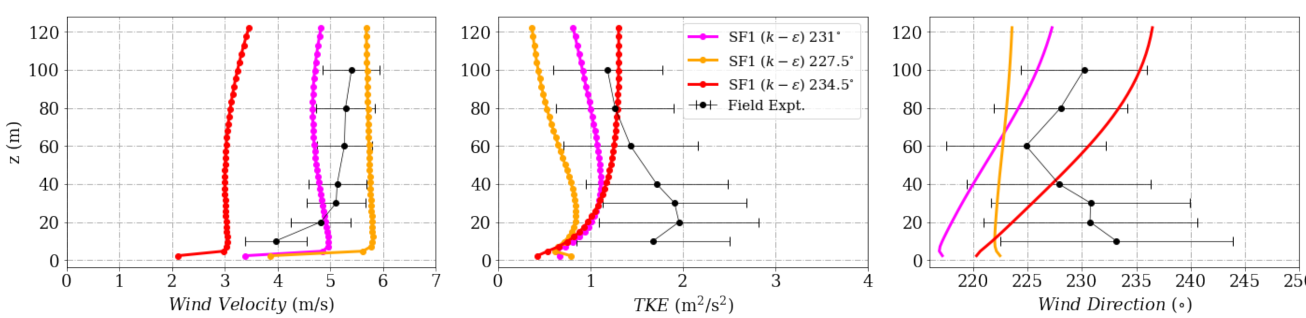

Figure 8: Simulation results and experimental data for wind velocity on the Northeast ridge for Tower 29 (tse13) for the SF1 ($k-\epsilon$) model.

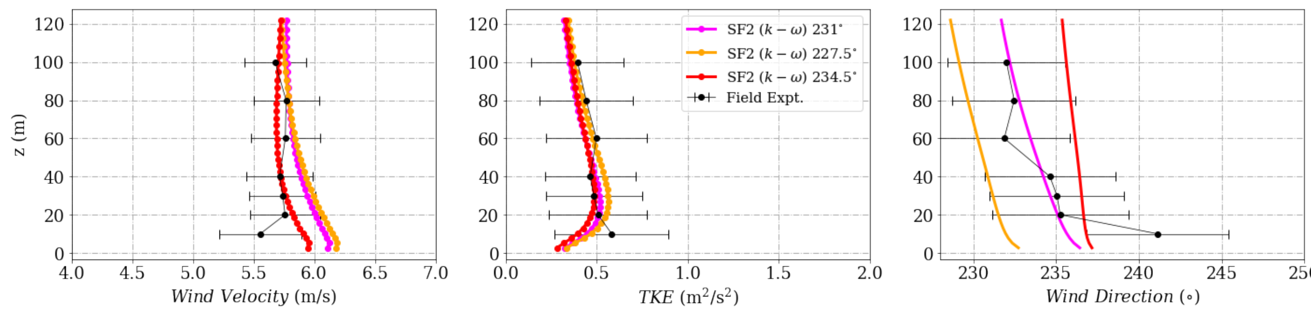

Figure 9: a) Wind velocity magnitude b) Wind direction c) Turbulent kinetic energy tuned to reach calibration at height 573 m corresponding to 100 m at Tower 20 (tse04) for the SF2 ($k-\omega$) model.

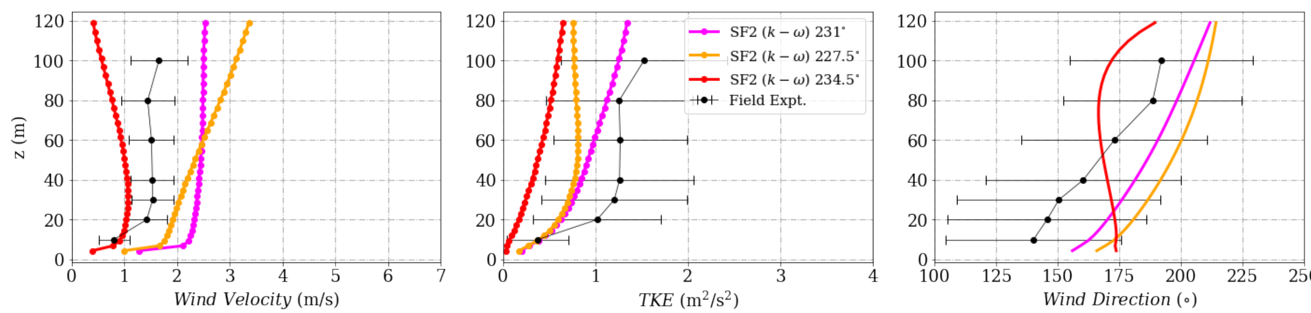

Figure 10: a) Wind velocity magnitude b) Wind direction c) Turbulent kinetic energy at Tower 25 (tse09) for the SF2 ($k-\omega$) model.

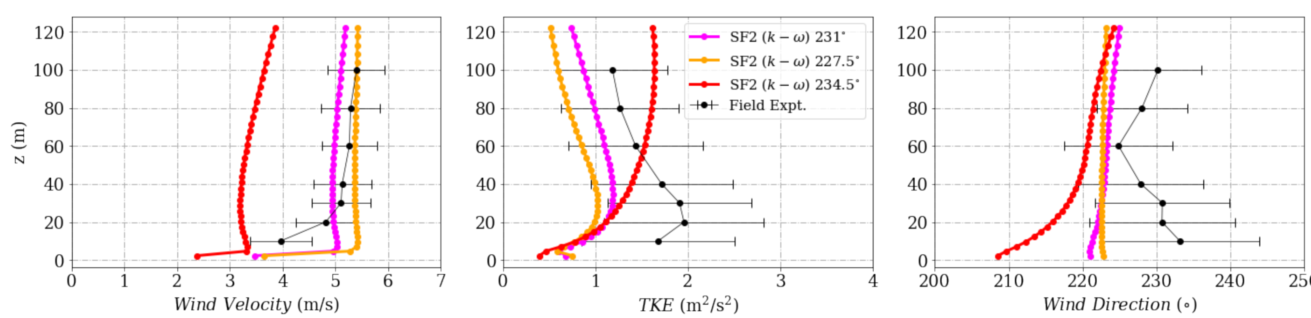

Figure 11: a) Wind velocity magnitude b) Wind direction c) Turbulent kinetic energy at Tower 29 (tse13) for the SF2 ($k-\omega$) model.

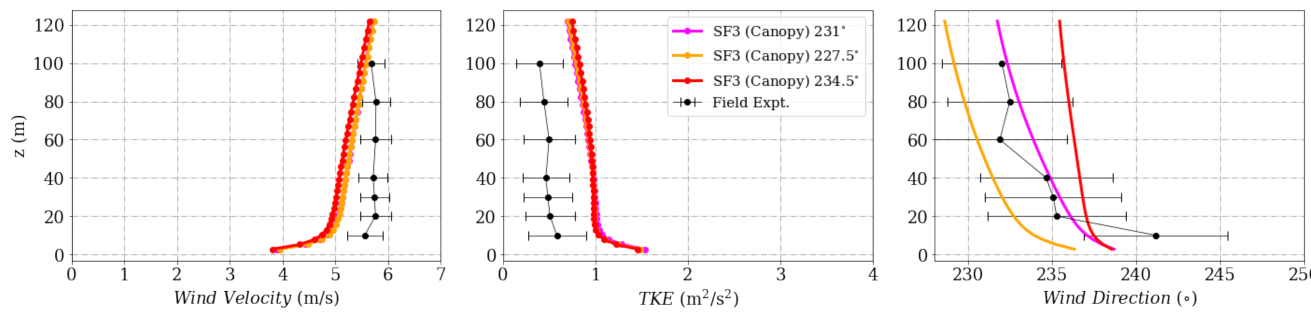

Figure 12: a) Wind velocity magnitude b) Wind direction c) Turbulent kinetic energy tuned to reach calibration at height 573 m corresponding to 100 m at Tower 20 (tse04) for the SF3 (Canopy) model.

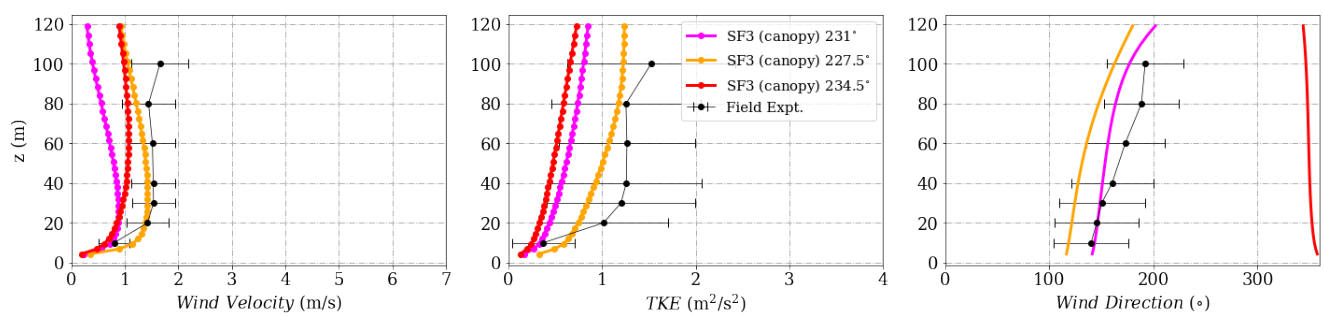

Figure 13: a) Wind velocity magnitude b) Wind direction c) Turbulent kinetic energy at Tower 25 (tse09) for the SF3 (Canopy) model.

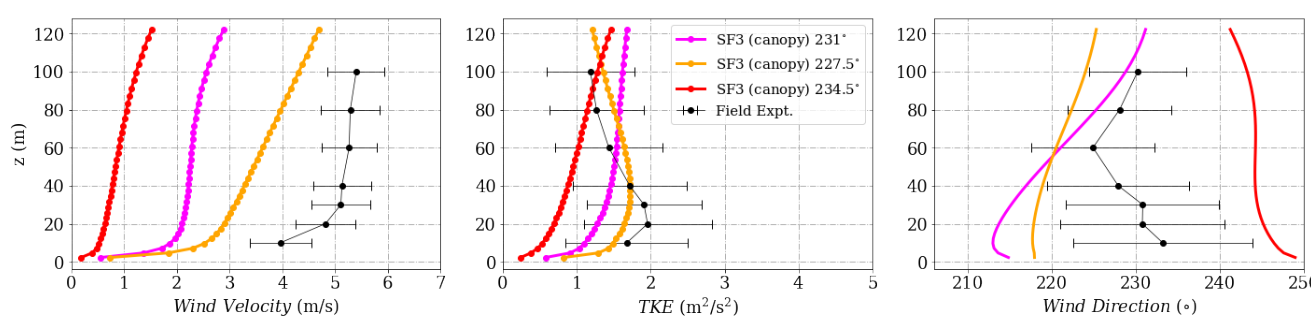

Figure 14: a) Wind velocity magnitude b) Wind direction c) Turbulent kinetic energy at Tower 29 (tse13) for the SF3 (Canopy) model.

4 SF4 Coriolis

The influence of wind direction change using the SF3 (Coriolis) source term model at different towers is shown in Figs 15, 16 and 17 respectively. Interestingly, for this case, the flow difference between the 231° and the 234.5° degree cases at Towers 25 and 29 is relatively small compared to the SF1 $k-\epsilon$ case. With the Coriolis source term, the flow turning due to the Coriolis effect is accounted for, and hence the inflow wind for calibration is set accordingly to obtain the required wind direction at the calibration mast. Consequently, the path taken by the wind across the terrain is different.

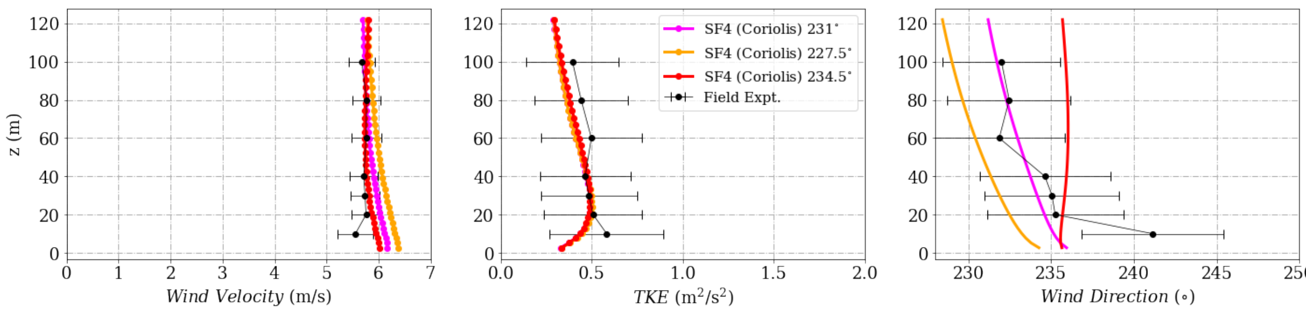

Figure 15: a) Wind velocity magnitude b) Wind direction c) Turbulent kinetic energy tuned to reach calibration at height 573 m corresponding to 100 m at Tower 20 (tse04) for the SF4 (Coriolis) model.

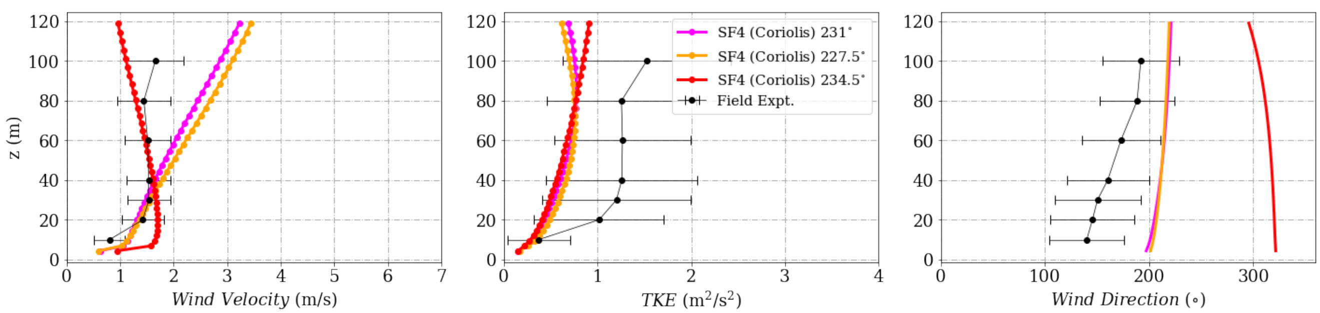

Figure 16: a) Wind velocity magnitude b) Wind direction c) Turbulent kinetic energy at Tower 25 (tse09) for the SF4 (Coriolis) model.

5 BBSF

Figs 18,19 and 20 show the wind profiles for the BBSF simulation model with the precursor inflow. Here the inflow from wind direction 234.5° shows a larger difference between the bother profiles even at the calibration mast, and a decrease in wind velocity at Tower 29 on the North-East Ridge, similar to the other models. The wind direction standard deviation bounds in Fig 20 appear to be more closely predicted by this model.

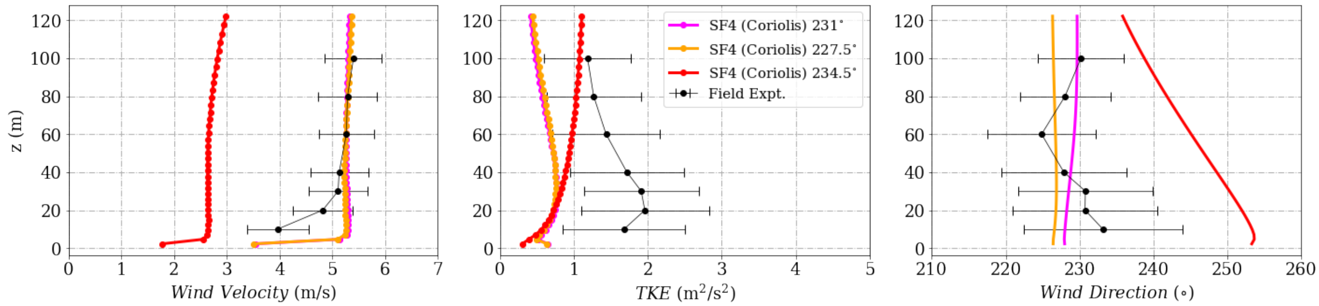

Figure 17: a) Wind velocity magnitude b) Wind direction c) Turbulent kinetic energy at Tower 29 (tse13) for the SF4 (Coriolis) model.

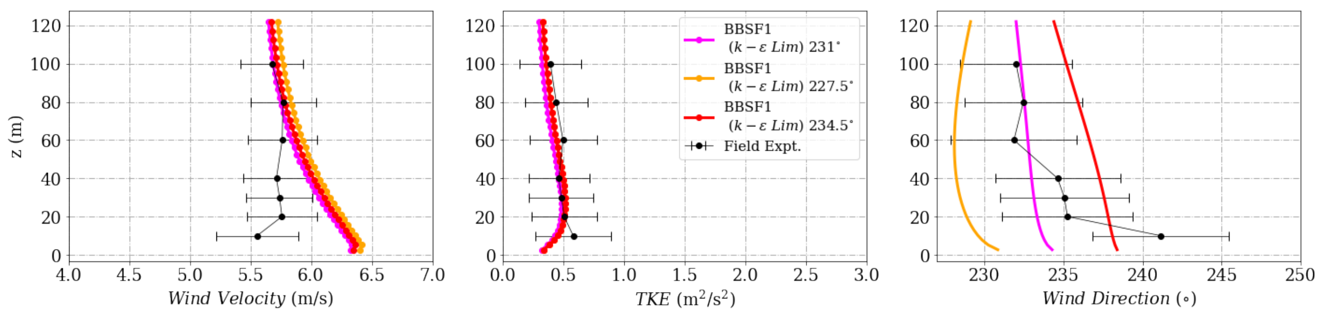

Figure 18: a) Wind velocity magnitude b) Wind direction c) Turbulent kinetic energy tuned to reach calibration at height 573 m corresponding to 100 m at Tower 20 (tse04) for the BBSF model.

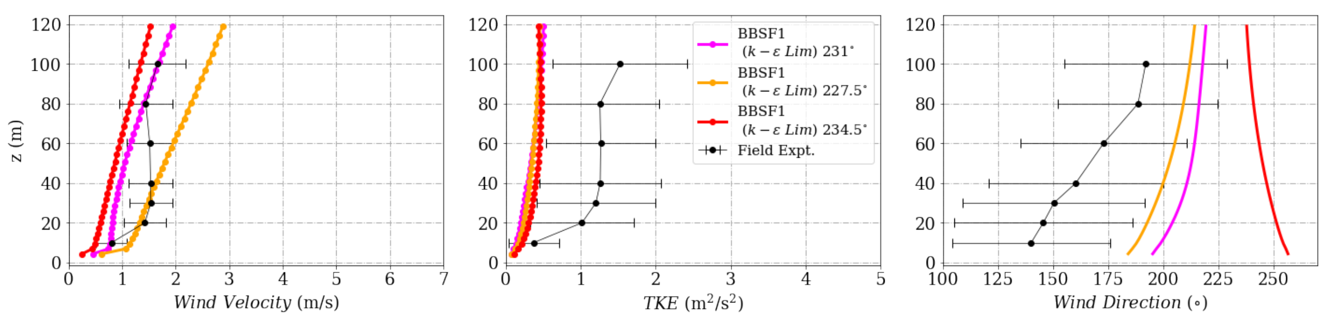

Figure 19: a) Wind velocity magnitude b) Wind direction c) Turbulent kinetic energy at Tower 25 (tse09

for the BBSF model.

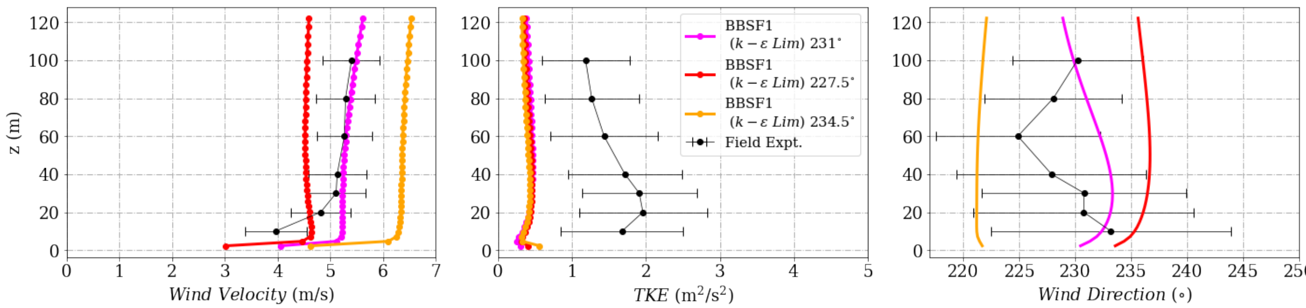

Figure 20: a) Wind velocity magnitude b) Wind direction c) Turbulent kinetic energy at Tower 29 (tse13) for the BBSF model.

References

[1] Jose Laginha Palma et al. "The digital terrain model in the computational modelling of the flow over the Perdigão site: the appropriate grid size". In: *Wind Energy Science* 5 (Nov. 2020), pp. 1469–1485. DOI: `10.5194/wes-5-1469-2020`.

[2] Jonas Schmidt, Carlos Peralta, and Bernhard Stoevesandt. "Automated generation of structured meshes for wind energy applications". In: London: Open Source CFD International Conference, London, Oct. 2012.